ARCING in LEO and GEO SIMULATED ENVIRONMENTS: COMPARATIVE ANALYSIS

Boris V. Vayner*
Ohio Aerospace Institute, Cleveland, Ohio 44142
Dale C. Ferguson♣
NASA Marshall Space Flight Center, Huntsville, Alabama 35812
and
Joel T. Galofaro♠
NASA John H. Glenn Research Center at Lewis Field, Cleveland, Ohio 44135

Comprehensive tests of two solar array samples in simulated Low Earth Orbit (LEO) and Geosynchronous Orbit (GEO) environments have demonstrated that the arc inception voltage was 2-3 times lower in the LEO plasma than in the GEO vacuum. Arc current pulse wave forms are also essentially different in these environments. Moreover, the wide variations of pulse forms do not allow introducing the definition of a "standard arc wave form" even in GEO conditions. Visual inspection of the samples after testing in a GEO environment revealed considerable damage on coverglass surfaces and interconnects. These harmful consequences can be explained by the discharge energy being one order of magnitude higher in vacuum than in background plasma. The tests also revealed a potential danger of powerful electrostatic discharges that could be initiated on the solar array surface of a satellite in GEO during the ignition of an arcjet thruster.

Nomenclature

C = capacitance, F
E = electric field strength, $V*m^{-1}$
I_m = arc current amplitude, A
N = number of atoms
S = surface area, m^2
T_e = electron temperature, eV
T_i = ion temperature, eV
U = voltage, V
V_b = electron beam energy, eV
V_{sc} = second crossover energy, eV
V = plasma speed, $m*s^{-1}$
$d_{1,2}$ = coverglass and adhesive thickness, m
j = current density, $A*m^{-2}$
n_e = electron number density, m^{-3}
n_i = ion number density, m^{-3}
r = arc rate, s^{-1}
t = time, s
δ = secondary electron emission yield,
$\varepsilon_{1,2}$ = dielectric constant of coverglass and adhesive
σ = conductivity, $(Ohm*m)^{-1}$
τ = pulse width, s

*Senior Scientist; vayner@grc.nasa.gov, Member AIAA.

♣ Senior Physicist, Environmental Effects Branch, Senior Member AIAA.

♠ Physicist, Photovoltaic and Space Environment Branch, Member AIAA.

1. Introduction

The launching of a spacecraft into any orbit demands a profound preliminary investigation of the interactions of the spacecraft with the natural space environment. One of many issues is differential electrostatic charging of spacecraft elements that may cause potentially detrimental electrostatic discharge (ESD). Physical mechanisms of differential charging are different for spacecraft in Low Earth Orbit (LEO) and in Geosynchronous Orbit (GEO) but the final result of charging is the same for both orbits: a very strong electric field generated in the vicinity of a conductor-dielectric junction. When the electric field strength exceeds some critical magnitude ESD is initiated, with possible negative consequences for further spacecraft function[1-4]. In order to prevent ESD on spacecraft surfaces or to mitigate negative consequences of ESD that cannot be averted, two consecutive actions are usually taken by spacecraft designers: 1) computer simulations of spacecraft charging to allow determination of areas with the highest electric fields; 2) ground tests of the respective spacecraft elements in simulated LEO or GEO environments. Technically, despite the same purpose of generating a high electric field in the area of a conductor-dielectric junction, experimental setups and tools are very different for LEO and GEO simulated environments. Testing in simulated LEO conditions has such advantages as more controllable charging, less time consumption, and lower equipment costs. If the arc threshold magnitudes of electric field strengths

were equal in LEO and GEO environments future tests could be performed in a simulated LEO plasma only. To verify the suggested possibility of making the tests easier, two solar array coupons were tested in both simulated environments, and the results were compared to each other and to theoretical estimates of ESD inception voltages. Unfortunately, the answer is negative, and the reasons for that are detailed below.

II. Experimental Setup

Two coupons were chosen for comparative tests in LEO and GEO simulated environments. Both coupons consist of three strings each with twelve 4x6 cm silicon cells in a string. Coverglass thicknesses are the same for both coupons (150 μm) but one has ultraviolet resistant (UVR) ceria-doped (CMX) coverglass while the other one has UVR borosilicate glass. These solar array samples had been previously tested under simulated LEO conditions[5,6]. For testing in a GEO environment, both coupons were vertically mounted in a horizontal vacuum chamber (the "Tenney" chamber) equipped with a high-speed cryogenic pump. An electron gun (EG) installed on the chamber door provided an electron beam with adjustable energy and emission current. Our chamber dimensions allowed mounting coupons at a distance of 1.3 m from the EG orifice, which delivered a satisfactory uniform flux over a 45 cm diameter circle. A non-contacting electrometer (Trek probe) was used to measure the surface potential distribution on both coupons (Fig.1). A strong electric field across the coverglasses was generated by applying a high negative voltage (-1.1 kV) to all strings and irradiating the front surfaces with the electron beam. Due to emission of secondary electrons from a coverglass, its potential becomes more positive than the potential of the interconnect and semiconductor; thus, so-

called inverted gradient conditions are created. These conditions are similar to those in a LEO plasma in the sense of the electric field strength and direction.

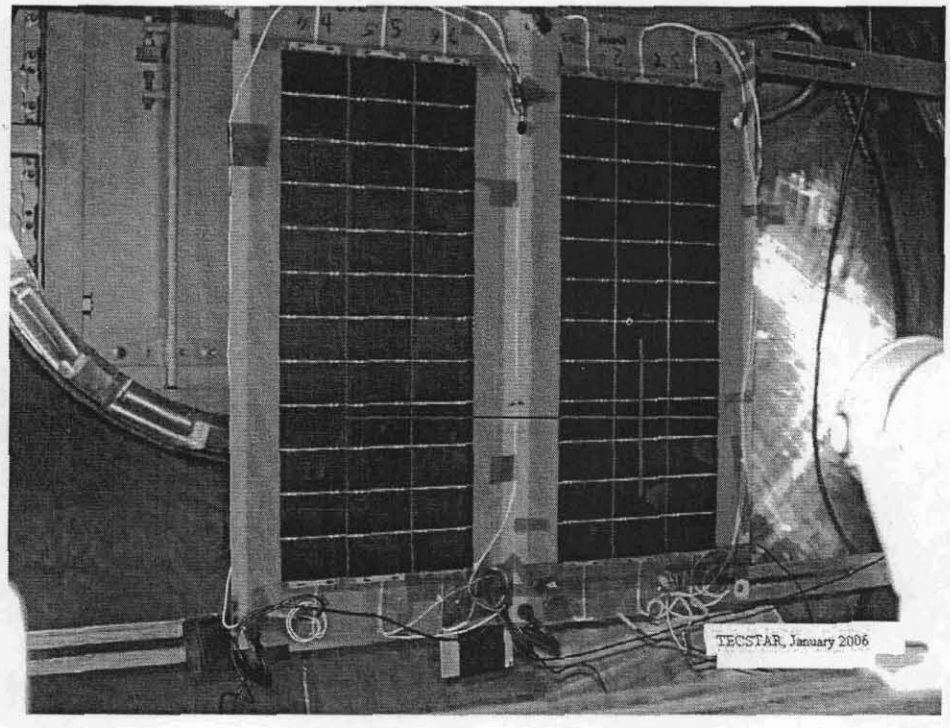

Fig.1. Two coupons are shown installed in the Tenney chamber. Crossed lines indicate area available for the Trek probe scan.

Arc current pulses were registered by three current probes, and all wave forms were stored on a PC's hard drive for further analysis. One spherical Langmuir probe (LP) of 1.9 cm diameter was installed at the distance of 0.9 m from the center of the cross in Fig.1 and connected to an oscilloscope with 50 ohm coax cable. The signal from this probe was used just to determine plasma behavior during discharge development (Fig.2). The arcing site locations were determined by employing a color video camera and video cassette recorder. All tests were done at room temperature.

III. ESD initiation

The basic theory of ESD inception in the area of conductor-dielectric junction was developed about fifteen years ago[7-9], and the main conclusion was that the arc site is a small spot on a conductor surface with a very high electric field enhancement due to a geometrical factor (such as a protrusion). The high electric field may cause cold cathode electron emission from this spot, the emitted electrons charge a side surface of a dielectric, resulting in further field enhancement and an increase in emitted current and spot temperature, and at some point this chain of events becomes an avalanche-like process revealing itself in a short current pulse and a bright flash of light. The temperature of the metal protrusion rises above its melting point, and a metal plasma is ejected into the surrounding space. This general picture was confirmed by observations of metal (usually silver) spectral lines[10-12] and correlations between intensities of UV emission and arc current pulse wave forms[13].

The electric field normal to the coverglass surface has a magnitude

$$E = \frac{\varepsilon_1}{\varepsilon_2 d_1 + \varepsilon_1 d_2}\left(\Phi_{cg} - U_b\right) \qquad (1)$$

In simulated LEO conditions the coverglass floating potential is close to the plasma potential, and usually does not exceed a few volts. Thus, the electric field strength is entirely determined by the bias voltage ($U_{pl} << U_b$), and an estimate $E \approx 1.5$ MV/m of the arcing threshold holds well for samples under the current test[5]. On both samples arcing was initiated at bias voltages U_b=300 V, and this magnitude could be considered as approximately equal to the threshold voltage. In simulated GEO conditions the situation is more complicated[14]. If the electron beam energy exceeds the bias voltage ($V_b > |U_b|$),

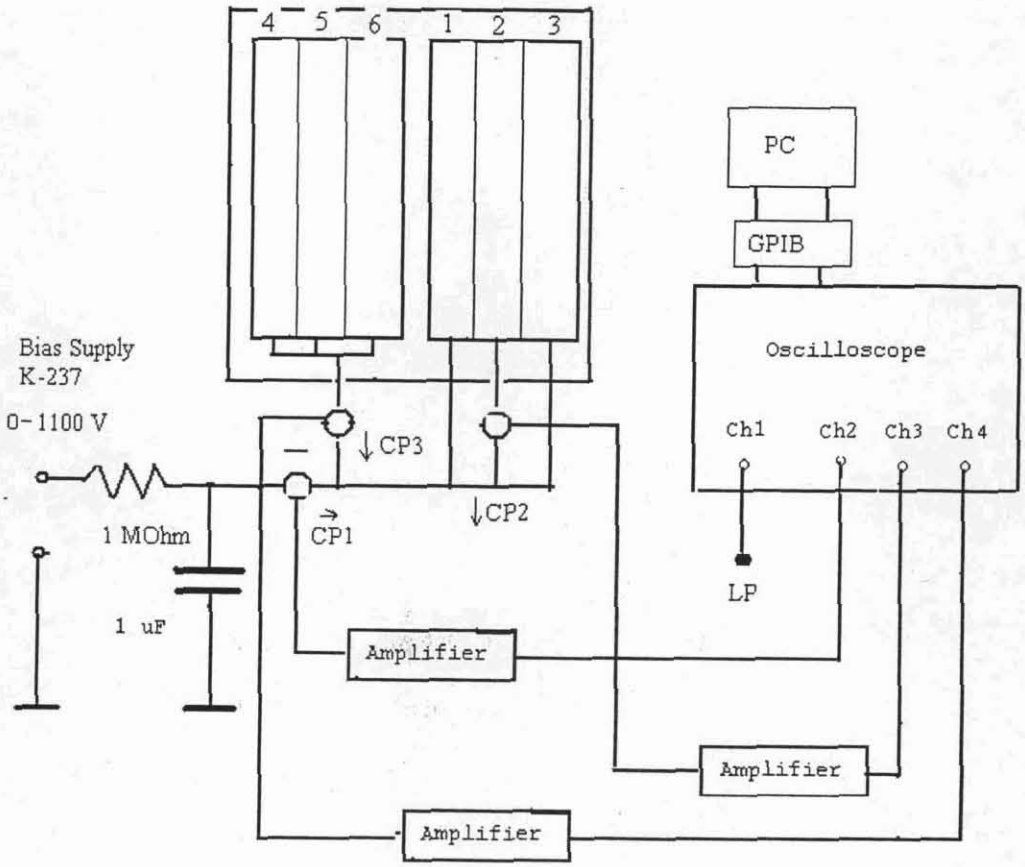

Fig.2. Circuitry diagram for registering current and LP potential pulse wave forms.

electrons strike the coverglass surface and generate secondary electrons. At the beam energies, the secondary electron emission (SEE) yield is higher than one, and the surface charges positively to a potential nearly equal to V_b-V_{sc}. It is commonly believed that the magnitude of the "second crossover" energy is higher than 2 keV for any dielectric material used as coverglass for solar arrays[14-17]. However, the SEE yield depends on many other parameters that are practically uncontrollable during an arcing test. For example, the process of charging itself causes a factor-of-two drop in SEE yield in a fraction of a second, but the time interval between consecutive ESDs exceeds minutes[18] .

Surface contamination and the presence of other dielectric materials (Kapton and adhesive in the gap between cells) influence the total SEE yield also.

From previous tests of these samples[6], the arc inception voltage is expected to be higher than 300 V, which means that the surface potential must reach magnitudes above 700 V negative. In an attempt to find the arc threshold voltage in simulated GEO conditions, a low bias voltage and low beam energy were used. Even though differential charging depends on the difference between bias voltage and beam energy

$$\Phi_{cg} - U_b = V_{sc} - V_b - U_b \qquad (2)$$

employing the EG with V_b<5 keV brings such disadvantages as a low ratio of beam current to emission current and a non-uniform distribution of current density across the beam. However, the surface potential distribution is quite uniform and was accepted for the purpose of determining the arc inception voltage.

During this particular test (Fig.3), differential charging was stabilized on the level of 600-700 V, and was kept steady for 25 minutes when no arc occurred. An effective "second crossover" energy can be determined from these data to be V_{sc}=1.6-1.7 kV. It is interesting to compare the magnitudes of this parameter obtained by different research groups. Irradiating a small array sample with a 2.5 keV beam resulted in charging the coverglass surface to the potential of 1.3-1.6 kV negative[19]. Thus, this estimate for the "second crossover" energy is 0.9-1.2 kV, well below the theoretical predictions of over 2 kV. Another group[20] used an electron beam energy of 5.3 keV, resulting in charging the surface up to a potential of -4 kV, which means that the "second crossover" point amounted to 1.3 kV. In another series of tests[21] the sample was irradiated with a 9 keV electron beam, charging the surface up to 5 kV negative. These measurements indicate a

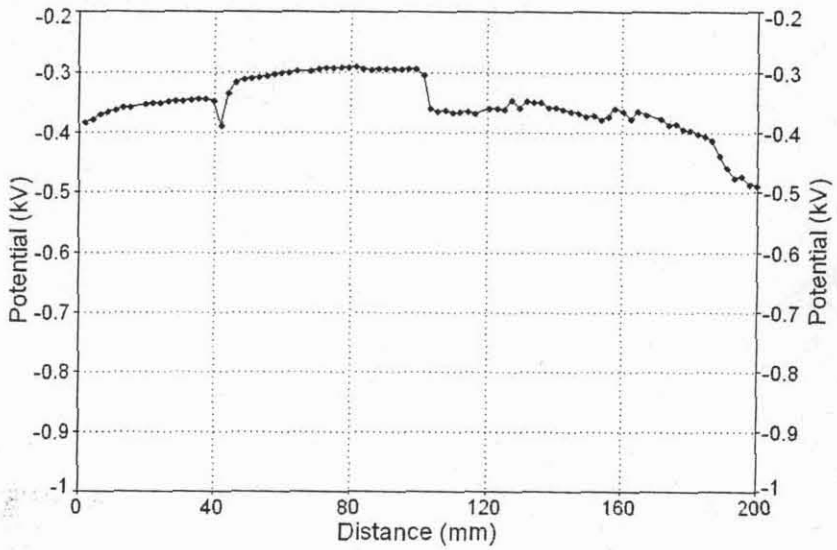

Fig.3. Surface potential distribution measured along the horizontal axis after 10 minute irradiation with a 2 keV electron beam. Bias voltage -1.0 kV. Distance was measured from the right-hand edge of scanned area (see Fig.1).

much higher "second crossover" of 4 kV. It is seen from these data that a general trend can be expressed as the following: a higher electron beam energy yields a higher estimate for the "second crossover". Moreover, in the final tests mentioned above[21], the differential charging reached 3 kV, too high for the purpose of searching for the arc inception voltage for the samples under our present test.

In our tests, the first arc took place on the interconnect between cells #6 and #7 on string #2 (Fig.4). In order to initiate this ESD about one hour of irradiation was needed. First, the sample was biased to 1.1 kV negative and irradiated with an electron beam (1.8 keV) for twenty two minutes, when a steady regime was established. Then, the EG was turned

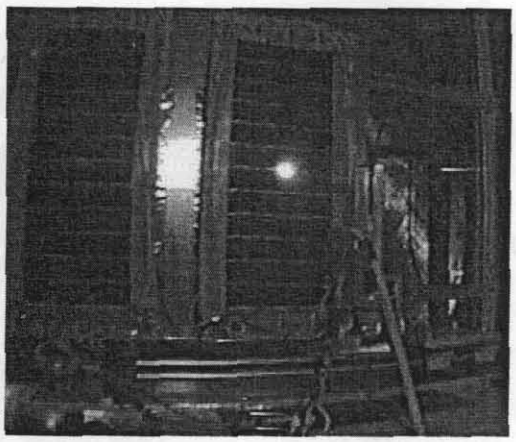

Fig.4. Image of the arc initiated by irradiation of the sample with the 1.8 keV electron beam. Bias voltage 1.1 kV negative, and differential charging 850 V.

off and the surface potential distribution was measured for about 3 minutes. Potentials varied between -320 V (string #3) and 250 V (strings # 1 and #2). The EG was turned on again, and after twenty four minutes of irradiation the discharge occurred. Immediately after this event the EG was turned off, and the surface potential distribution was measured again. The results of these measurements demonstrated that the surface had been fully discharged: potentials varied between -1040 V on string #3 and -970 V on string #1. The second arc under the same conditions took place in the gap between strings #1 and #2 at the level of the second cell from the bottom. This arc caused malfunctioning of the Trek probe, and the potential distribution was not measured after this particular event.

Now it is possible to derive the threshold electric field strength as E_{th}=4 MV/m (Eq.1). One of the reasons for this field to be much higher than the threshold field strength in simulated LEO conditions may be the absence of the additional field enhancement due to coverglass side-surface charging in a LEO plasma[22]. Actually, in a xenon plasma the ion current density on the interconnect surface can be roughly estimated as

$$j_i = j_{i0}\frac{U_b}{T_i} \qquad (3)$$

The ions striking the metal surface create a secondary electron current with the density[9]

$$j_i = j_{i0} \cdot \delta_i \qquad (4)$$

The magnitude of the secondary electron emission yield is about $\delta_i \approx 10^{-2}$, and for a simulated LEO plasma with $n_i = 10^6 cm^{-3}$ and T_i =0.03 eV the electron current toward the coverglass side-surface can reach 100 nA/cm^2. The EG used in our test provided a beam current density of about 1 nA/cm^2 perpendicular to the coverglass surface, and certainly much less flux to the side surface. This flux cannot be high enough to charge the side surface because of coverglass conductivity. A conductive current density is estimated as

$$j_c = \sigma_g \cdot E \qquad (5),$$

and this current density can get to 0.4 nA/cm^2 when electric field is close to its threshold magnitude.

Another (or additional) factor contributing to the higher arcing threshold electric field under GEO simulated conditions can be electron impact desorption (EID), which plays a significant role in ESD initiation in a plasma[5,10] and is strongly suppressed in GEO vacuum conditions.

Whatever is the reason for the discrepancy, the experimental data confirm with a high degree of certainty that the arc initiation voltage is 2-3 times higher in GEO than in LEO simulated conditions.

IV. Arcing in Vacuum

In order to provide a chance for straight comparison of arc parameters in the previous LEO plasma test[6] and the present GEO vacuum test, an additional capacitor of 1 μF was installed between solar array sample and the ground (Fig.2). This capacitance is much higher than the capacitance of the sample (700 pF/string), and its correct magnitude has been under discussion for a long time[20,21,23-26]. However, there is currently a general agreement that at least 1 m^2 of solar array area will be fully discharged by an arc on its surface, and that is equivalent to discharging a 0.25 μF capacitor. If one takes into account the capacitance of other spacecraft elements that can supply additional current to the discharge, the adopted value of 1 μF looks quite reasonable.

After establishing the threshold value for differential charging and removing the diaphragm from the EG's orifice to allow irradiating a larger area, the arc parameters were studied by initiating arcs and measuring current pulse wave forms. The first event was located on the interconnect between cells #3 and #4 (from the top) on string #6. It is seen in Fig.5 that the current through the arcing string (CP3) is practically equal to the capacitor discharge current. The small difference between these two currents at the end of the discharge could be attributed to current passing through another coupon.

Unfortunately, a scale for the respective channel was chosen incorrectly, and probe CP2 did not register any signal. The current amplitude reached 50 A, and this could lead to failure of the entire string. The pulse width (~ 30 μs) was approximately equal to the widths measured for discharges in LEO plasma conditions. A crude estimate for the lost charge

$$\Delta q = \frac{I_m \tau}{2} = 1000 \ \mu C \qquad (6)$$

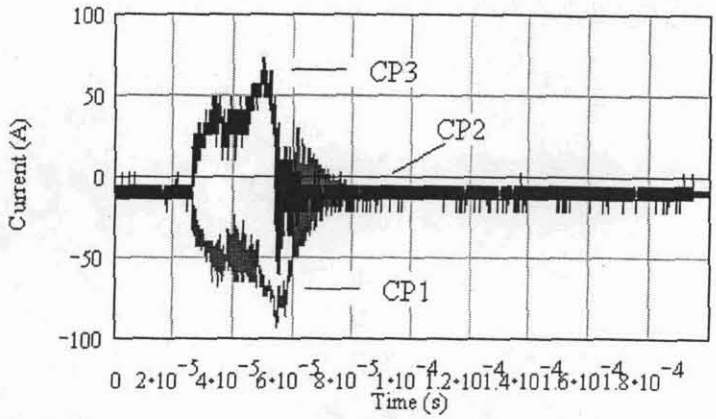

Fig.5. Arc currents are shown for the ESD event on the string #6. EG beam energy 1.8 keV and bias voltage -1.1 kV.

is in general agreement with the initial charge on the capacitor (~1100 μC).

The next arc occurred on string #3 (between cells #1 and #2 from the bottom). It is seen in Fig.6 that this discharge needed much more time to develop. Scanning the sample with the Trek probe revealed practically full neutralization of all the positive charge stored on coverglass surfaces. Taking into account the limited area irradiated by the electron beam (about twenty cells on the left coupon) one can estimate the ratio of capacitances

$\frac{C_s}{C} = 10^{-3}$, which corresponds very well with the ratio of lost charges calculated from the current pulse measurements (see Fig.6).

For the next stage of the test, the EG was turned off and a xenon (LEO type) plasma was generated to verify the arcing parameters. The whole sample was biased -300 V, and the arc rate was

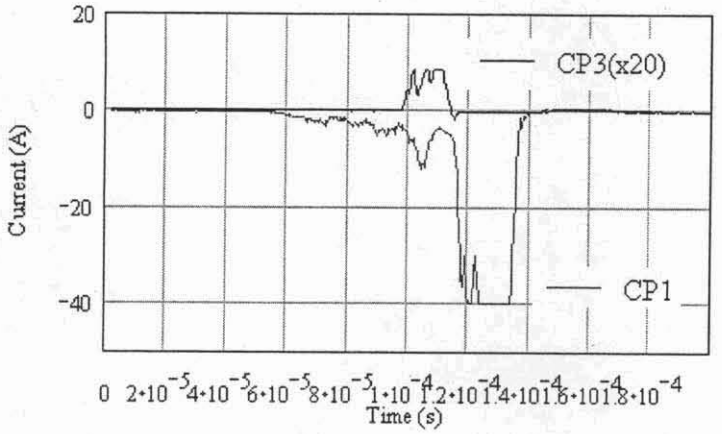

Fig.6. Arc currents are shown for the ESD event on the string #3. EG beam energy 1.8 keV and bias voltage -1.1 kV.

determined to be r=0.25 arcs/min.

Five more arcs were generated under simulated GEO conditions with essentially the same results as discussed above. Comparison between arc current pulse wave forms for arcs in GEO and LEO simulated conditions showed some differences: arcs in the GEO vacuum developed slower than in the LEO plasma, and they showed "oscillations" on the rising part of the pulse. These observations seem to be important for understanding the physical processes in the discharge development[20,21].

V. Plasma Generated by the Arcs

When a discharge occurs, an electric current flows through the conductive plasma produced by the discharge itself. This plasma originates from melting and evaporation of metal from the spot on the cathode (interconnect) surface[27,28]. Both solar array samples under study have silver-plated interconnects. According to Anders[29] the arc plasma consists mainly of silver ions with an average charge Q_{Ag}=2.14 and electrons with a temperature T_e≈4 eV. A typical discharge provides about N_i= 5*10^{15} Δq ions that are

ejected into the chamber during a 50-100 μs time interval[29]. A rough estimate for the ion number density in vacuum chamber can be obtained from the following equation

$$n_i = \frac{N_i}{\tau \cdot V \cdot S} \qquad (7)$$

Substituting Eq.6 into Eq.7 and using $V=10^6$ cm/s for the ion velocity[30], one can get $n_i \geq 10^6$ cm^{-3}. This magnitude exceeds the ion number density in the background plasma for simulated LEO conditions. It is interesting to compare a Langmuir probe response to the arc in vacuum and in plasma (Fig.7). These graphs illustrate also the main difference between arc current pulse wave forms for both test conditions.

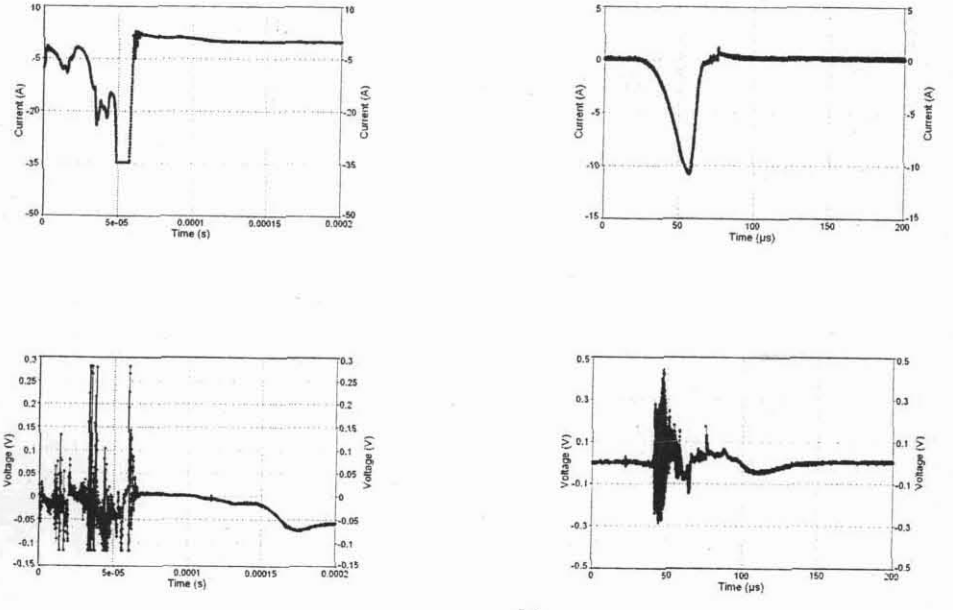

a) b)

Fig.7. Arc current and LP potential measured in a) vacuum and b) LEO plasma.

These measurements were performed with time resolution Δt=40 ns. No measurable delay between the arc initiation and LP response was found in either case. It is seen in

Fig.7 that the arc current pulse in a (GEO) vacuum has a long lasting front with clearly expressed oscillations, and the current drops sharply to zero when the arc extinguishes because the capacitor is fully discharged. The (GEO) test performed in Ref. 21 revealed essentially different arc current behavior: a sharp front and slowly decreasing current without any oscillations. Another test[20] demonstrated pulses with sluggish front and slow dropping current with some oscillations. We do not have an explanation for the described discrepancies, but in both tests[20,21] the external capacitance was much less and the sample size was much higher than in our present test. However, two pulses among twenty measured in the present experiment also possessed features observed in Refs. 20 and 21 (Fig.8). This fact creates doubts regarding the ability to define any such thing as a "standard pulse." The LP responses to the arc plasma are practically identical in vacuum and simulated LEO conditions (Fig.7). In both cases the LP floating potential reaches -0.05 V after the period of oscillations with an amplitude of around 0.3 V.

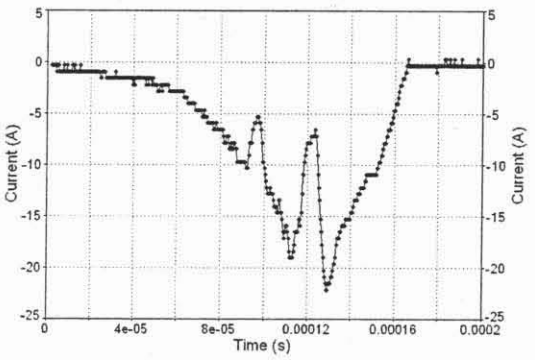

Fig.8. Arc current pulse registered after 3 minutes irradiation with the beam of 1.5 keV energy.

VI. Transitional Processes

Spacecraft in GEO generally employ arcjet thrusters for station keeping. The number of thrusters and their spatial positions relative to the solar panels depend on the spacecraft type, but for a qualitative analysis one can adopt a distance of a few meters and a thruster power of a few kilowatts. While in operation the thruster ejects a weakly ionized plasma that surrounds the solar array and makes it operate in conditions close to those in a LEO environment. That is why it is reasonable to simulate this stage of spacecraft operation in a plasma chamber filled with a noble gas[31]. A full scale test[32] revealed plasma parameters n_e=10^6-10^7 cm^{-3} and T_e=0.1-02 eV at a distance of a few meters from the nozzle of a 2 kW arcjet thruster. However, these tests left unanswered the question of the transitional processes caused by enveloping a previously charged in GEO environment solar array with a consequently neutral gas and plasma.

In order to simulate transitional processes, the sample was biased to -1.1 kV and charged with the EG, and then the flow of Xenon gas was initiated into chamber. A discharge occurred within a few seconds (Fig.9). The arc current pulse wave form resembles one in a LEO environment. The pulse is short, and the current amplitude exceeds 50 A. This experiment was repeated three times with the same results.

Thus, this test clearly demonstrates that GEO spacecraft charged to high negative potential may experience ESDs on solar array surfaces during the short period of time while initiating an arc jet operation. ESDs can be also initiated on a spacecraft in polar orbit during the transition from the auroral zone to the low density LEO plasma region. The probability of an ESD event depends on the rate of spacecraft body potential variation, and an exact answer can be obtained by computer simulations and much more sophisticated tests in the future.

It is impossible to operate a Trek probe in the area of solar cells during EG operation. But, it seems useful to obtain data concerning the charging dynamics and potential changes

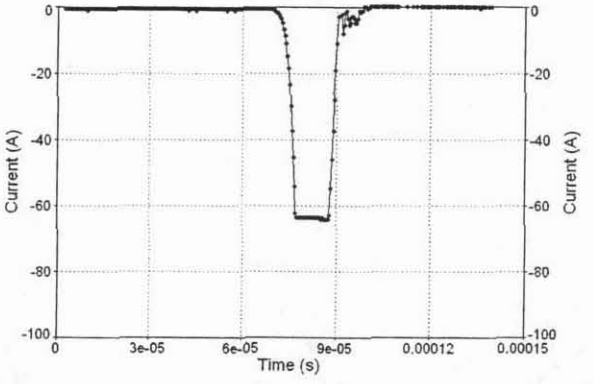

Fig.9. Discharge in a neutral gas (Xe) environment on the preliminary charged sample.

after the arc. The Trek probe was placed on the right edge of the sample (fiberglass surface, Fig.1) where the electron beam current density is minimal. This placement allows safe measurement of slow changes in surface potential and transients caused by an arc (Fig.10). The arc occurred on the string #2, and it is seen in Fig.10 that the arc plasma propagates far enough to discharge a significant portion of the sample surface.

Besides regular discharges with current pulse amplitudes of approximately 50 A, small flashes were observed on the sample surface. Visually these flashes are localized like regular arcs but their brightness is much lower. In most cases, the current pulse amplitudes were not high enough to trigger the oscilloscope but three events were registered with the peak currents about 1-1.5 A (Fig.11). During these discharges only

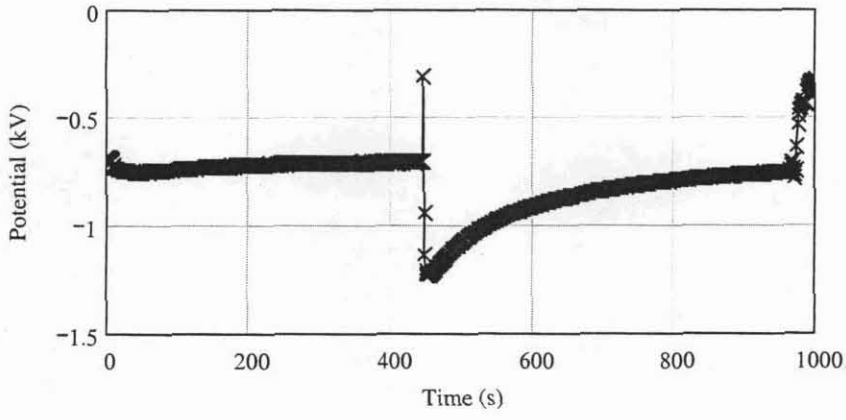

Fig.10. Surface potential measured by Trek probe in the far right position. ESD occurred at t=450 s. Trek probe started moving toward a solar cell at the moment t=950 s.

5% of the initial charge was leaked to the plasma. There were no measurable signals in other channels during this kind of events, and changes in surface potential were not registered.

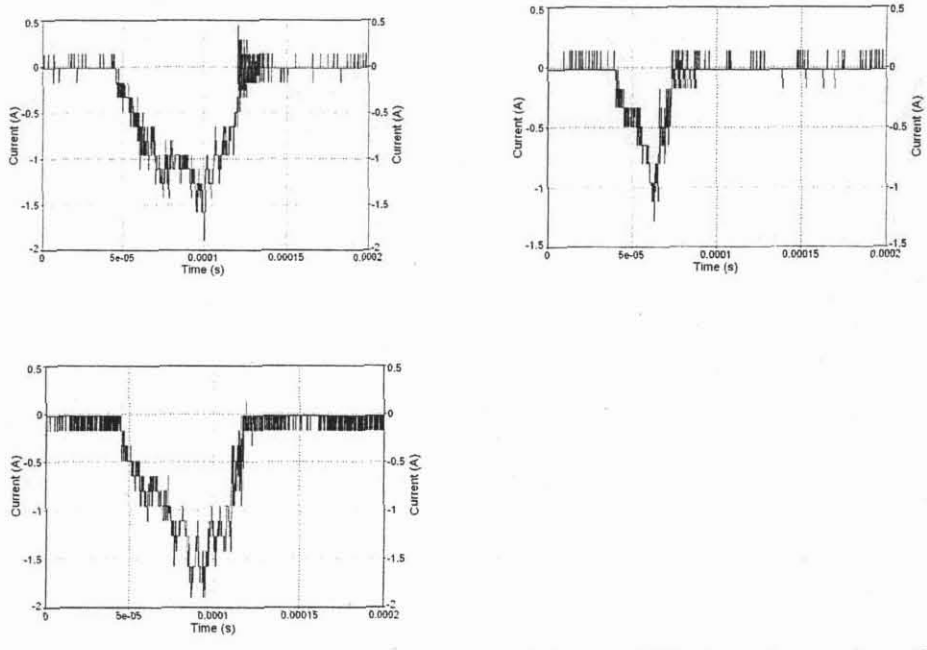

Fig.11. Current pulses in the Ch.2 (CP1) caused by small flashes observed on the sample surface irradiated with the 1.5 keV beam.

The current test was not particularly suited for measurements of plasma propagation speed. But, the wave forms of several events can be used to obtain rough estimates for the propagation of plasma along the sample surface and in vacuum toward the Langmuir probe. For example, the wave forms in Fig.12 were registered for the arc on string #3 between cells #1 and #2 from bottom. It is seen that the peak currents were registered by all three probes at the same time but the initiation of the discharge on the right sample was delayed by about 40 μs. If this delay was caused by the limited speed of plasma expansion the estimate for the speed was approximately 6 km/s. The pulse on the LP was delayed about 75 μs that allows estimating the plasma speed to be 12 km/s. Another estimate for the plasma expansion speed can be obtained from the current pulse width for the probe CP3. To discharge three strings (≈20 cm) during the time span of 20 μs the speed should be equal to 10 km/s. Statistical processing of data of eight events resulted in the following numbers: V=8.8±1 km/s if determined by the delay between the current pulse peak and the LP corresponding response, and V=9.9±2.2 km/s if the CP3 pulse width was used. All these numbers are in reasonable agreement with other measurements[20,21,33] but the method of plasma speed calculation certainly needs further development and clarification.

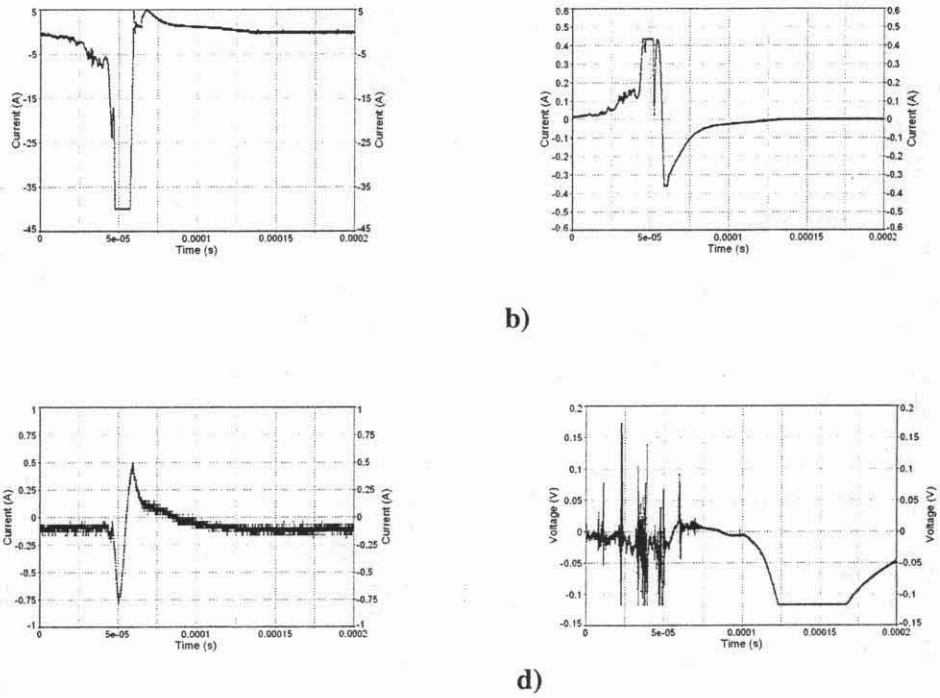

Fig.12. ESD on string #3: a) CP1; b) CP2; c) CP3; d)LP.

VII. Conclusions

Comprehensive tests of two solar array samples in simulated LEO and GEO environments have demonstrated that the arc inception voltage was 2-3 times lower in the LEO plasma. Arc current pulse wave forms are also significantly different in these environments. Moreover, wide variations of pulse forms did not allow introducing the definition of a "standard pulse" even in GEO conditions. In both tests an additional capacitor of 1 μF was installed between the sample and ground to provide current pulse amplitudes in the range of 25-50 A. The samples were visually inspected and photovoltaic I-V characteristics were taken after the test in the LEO environment. No damage was found after about hundred discharges experienced by each sample. The

visual inspection of the same samples after testing in the GEO environment revealed considerable damage on coverglass surfaces and interconnects (Fig.13). These harmful consequences can be explained by the discharge energy being one order of magnitude higher in the last (GEO) test. The test also revealed the potential danger of powerful ESD that could be initiated on solar array surfaces of GEO satellites during the ignition of an arc jet thruster.

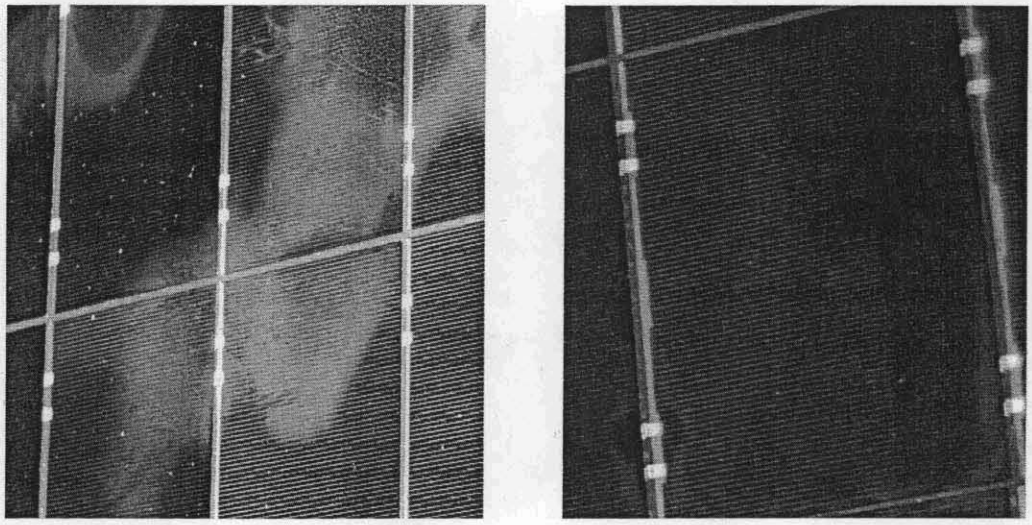

Fig.13. Examples of damages caused by arcing in simulated GEO environment.

Acknowledgment

Authors are greatly thankful to Mike Chornak for help with the experiment.

References

[1]Stevens, N.J. "Interaction Between Spacecraft and the Charge-Particle Environment", *Proceedings of Spacecraft Charging Technology Conference'*, NASA CP-2071, 1978, pp.268-294.

[2]Martin, A.R. "A Review of Spacecraft/Plasma Interaction and Effects on Space Systems", *Journal of The British Interplanetary Society*, Vol.47, 1994, pp.134-142.

[3]Hastings, D.E. "A Review of Plasma Interactions with Spacecraft in Low Earth Orbit", *Journal of Geophysical Research*, Vol.100, No.A8, 1995, pp.14,457-14,483.

[4]Garrett, H.B., and Whittlesey, A.C. "Spacecraft Charging, An Update", *IEEE Transactions on Plasma Science*, Vol.28, No.6, 2000, pp.2017-2028.

[5]Vayner, B., Galofaro, J., and Ferguson, D. "Interactions of High-Voltage Solar Arrays with Their Plasma Environment: Physical Processes", *Journal of Spacecraft and Rockets*, Vol.41, No.6, 2004, pp.1031-1041.

[6]Vayner, B., Galofaro, J., and Ferguson, D. "Interactions of High-Voltage Solar Arrays with Their Plasma Environment: Ground Tests", *Journal of Spacecraft and Rockets*, Vol.41, No.6, 2004, pp.1042-1050.

[7]Hastings,D.E., Weyl,G., and Kaufman, D. "Threshold Voltage for Arcing on Negatively Biased Solar Arrays", *Journal of Spacecraft and Rockets*, Vol.27, No.5, 1990, p.539-544.

[8]Cho,M., and Hastings, D.E. "Computer Particle Simulation on High-Voltage Solar Array Arcing Onset", *Journal of Spacecraft and Rockets*, Vol.30, No.2, 1993, pp.189-205.

[9] Jongeward, G., and Katz, I. "Effect of Conduction and Ion Current on Solar Array Arc Thresholds", *Proceedings of the 6th Spacecraft Charging Technology Conference*, Nov. 2-6, 1998, Air Force Res. Lab., Hanscom AFB, MA, USA, pp.42-46.

[10]Vayner, B., Galofaro, J., Ferguson, D., and Degroot, W. "Electrostatic Discharge Inception on a High-Voltage Solar Array", *AIAA Paper* 2002-0631, Jan.2002.

[11]Vayner, B., Galofaro, J., and Ferguson, D. "The Neutral Gas Desorption and Breakdown on Metal-Dielectric Junction Immersed in a Plasma", *AIAA Paper* 2002-2244, Jun.2002.

[12]Amorim, E., Levy, L., and Vacquie, S. "Electrostatic Discharges on Solar Arrays: Common Characteristics With Vacuum Arcs", *Journal of Physics D: Applied Physics*, Vol.35, 2002, pp.L21-L23.

[13]Upschulte, B.L., Marinelli, W.J., Carleton, K.L., Weyl, G., Aifer, E., and Hastings, D.E. "Arcing on Negatively Biased Solar Cells in a Plasma Environment", *Journal of Spacecraft and Rockets*, Vol.31, No.3, 1994, pp.493-501.

[14]Frederickson, A.R., Benson, C.E., and Cooke, E.M. "Gaseous Discharge Plasmas Produced by High-Energy Electron-Irradiated Insulators for Spacecraft", *IEEE Transactions on Plasma Science*, Vol.28, No.6, 2000, pp.2037-2047.

[15]Mueller, C.W. "The Secondary Electron Emission of Pyrex Glass", *Journal of Applied Physics*, Vol.16, No.8, 1945, pp.453-458.

[16]Krainsky, I., Lundin, W., Gordon, W.L., and Hoffman, R.W. "Secondary Electron Emission Yields", *Proceedings of the 3rd Spacecraft Charging Technology Conference*, Colorado Springs, CO, 1980, pp.179-197.

[17]Takahashi, M., Nishimoto, H., Kawalita, S., Cho, M., Nozaki, Y., Fujii, H., Murakami, Y., Ozaki, T., and Onodera, N. "ETS-VIII Solar PDL Plasma Interaction Problem Approach", *Proceedings of the 7th Spacecraft Charging Technology Conference*, Noordwijk, The Netherlands, 2001, pp.127-132.

[18]Dennison, J.R., Sim, A., and Thomson,C. "Evolution of the Electron Yield Curves of Insulators as a Function of Impinging Electron Fluence and Energy", *Proceedings of*

the 9th Spacecraft Charging Technology Conference, Tsukuba, Japan, 2005, pp.1-19.

[19]Cho, M., Ramasamy, R., Matsumoto, T., Toyoda, K., Nozaki, Y., and Takahashi, M. "Laboratory Test on 110-Volt Solar Arrays in Simulated Geosynchronous Orbit Environment", *Journal of Spacecraft and Rockets*, Vol.40, No.2, 2003, pp.211-220.

[20]Amorim, E., Payan, D., Reulet, R., and Sarrail, D. "Electrostatic Discharges on a 1 sq.m. Solar Array Coupon – Influence of the Energy Stored on Coverglass on Flashover Current", *Proceedings of the 9th Spacecraft Charging Technology Conference*, Tsukuba, Japan, 2005, pp.1-14.

[21]Leung, P. "Plasma Phenomena Associated with Solar Array Discharges and Their Role in Scaling Coupon Test Results to a Full Panel", *AIAA Paper* 2002-0628, Jan. 2002.

[22]Nevrovsky, V.A., and Ryl'skaya, L.A. "Limiting Electric Strength of Vacuum Electrode Systems Including Combined Breakdown", *Proceedings of the XXth International Symposium On Discharges and Electrical Insulation in Vacuum*, Tours, France, July 1-5, 2002, pp.190- 193.

[23]Ferguson, D.C., Vayner, B.V., Galofaro, J.T., and Hillard, G.B. "Arcing in LEO-Does the Whole Array Discharge?", *Proceedings of the 9th Spacecraft Charging Technology Conference*, Tsukuba, Japan, 2005, pp.1-11.

[24]Balmain, K.G., and Dubois, G.R. "Surface discharges on Teflon, Mylar, and Kapton", *IEEE Transactions on Nuclear Science*, Vol.26, No.12, 1979, pp.5152-5155.

[25]Snyder, D.B. "Characteristics of Arc Currents on a Solar Cell Array in a Plasma", *IEEE Transactions on Nuclear Science*, Vol.31, No.4, 1984, pp.1584-1587.

[26]Cho, M., Ramasamy, R., Hikita, M., Tanaka, K., and Sasaki, S. "Plasma Response

to Arcing in Ionospheric Plasma Environment: Laboratory Experiments", *Journal of Spacecraft and Rockets*, Vol.39, No.3, 2002, pp.392-408.

[27]*Handbook of Vacuum Arc Science and Technology*, Eds. R.L. Boxman, D.M. Sanders, and P.J. Martin. Noyes Publications, Park Ridge, NJ, USA, 1996, p.33.

[28]Mesyats, G.A., *Cathode Phenomena of Electric Arcs*, Nauka, Moscow, 2000, 375p.

[29]Anders, A. "Ion Charge State Distribution of Vacuum Arc Plasmas: The Origin of Species", *Physical Review E*, Vol.55, No.1, 1997, pp.969-981.

[30]Yushkov, G.Y., Anders, A., Oks, E.M., and Brown, I.G. "Ion Velocities in Vacuum Arc Plasmas", *Journal of Applied Physics*, Vol.88, No.10, 2000, pp.5618-5622.

[31]Cho, M., Ramasamy, R., Toyoda, K., Nozaki, Y., and Takahashi, M. "Laboratory Tests on 110-Volt Solar Arrays in Ion Thruster Plasma Environment", *Journal of Spacecraft and Rockets*, Vol.40, No.2, 2003, pp.221-229.

[32]Vayner,B., Galofaro, J., and Chornak, M. "Diagnostics of Low Temperature Hydrogen Plasma", *Proceedings of the 6th International Symposium Frontiers in Low Temperature Plasma Diagnostics*, Les Houches, France, 2005, p.81.

[33]Kim, J., Kawasaki, T., Sanmaru, Y., Hosoda, S., and Cho, M. "Influence of Coverglass on Primary Arc Propagation over GEO Satellite Solar Array", *AIAA Paper* 2006-0409, Jan.2006.